J. Condensed Matter Nucl. Sci. 6 (2012) 13–23

Research Article

Characterization of Neutrons Emitted during Pd/D Co-deposition

Pamela A. Mosier-Boss *
Research Laboratory of Electronics, MIT, Cambridge, MA 02139, USA

Frank E. Gordon †
Global Energy Corporation, Annandale, VA 22003, USA

Lawrence P.G. Forsley
JWK International Corp., Annandale, VA 22003, USA

Abstract

Experiments using CR-39 detectors have shown that energetic particles and neutrons are emitted during Pd/D co-deposition. Using 6 μm Mylar between the CR-39 and the cathode, it has been shown that the majority of the tracks formed have energies on the order of 1–3 MeV. This conclusion was supported by computer analysis of the pits using the 'Track_Test' program developed by Nikezic and Yu. In this communication, additional analysis of the detectors will be discussed. In particular, it will be shown that the size distribution of the neutron-generated tracks on the back side of the CR-39 detectors are consistent with the occurrence of DD and DT fusion reactions. This is supported by the presence of triple tracks in the CR-39 as well as the energies of the charged particles as determined in the Mylar experiments.

Keywords: Co-deposition, CR-39 detectors, Heterostructures, Photomicrographs, Triple tracks

1. Introduction

In the inertial confinement fusion (ICF) field, CR-39 is a solid state nuclear track detector (SSNTD) used to detect energetic particles such as alphas, protons, deuterons, and tritons as well as neutrons [1]. Because CR-39 is an allyl glycol carbonate plastic, it is not affected by the electromagnetic pulse (EMP) that disables electronic detectors in ICF experiments. When energetic charged particles travel into or through a CR-39 detector, they create along their ionization track a region that is more sensitive to chemical etching than the rest of the bulk. After treatment with an etching agent, tracks remain as holes or pits whose size and shape can be measured. The attributes that make CR-39

*E-mail: pboss@san.rr.com.
†Retired.

the detector of choice for ICF measurements also make it an ideal detector for detecting particle emissions in the Pd/D system. Also, since CR-39 detectors are examples of constantly integrating detectors, events are permanently stamped on and, in the case of neutrons, inside the detector. This is particularly important for systems, like Pd/D, that exhibit low flux rates and/or events that occur in bursts. Table 1 summarizes the strengths and weaknesses of SSNTDs [2].

Table 1. Strengths and Weaknesses of SSTDs [2].

Strengths	Weaknesses
Small geometry–trails of damage are nm/μm in diameter and length	Lack of real-time capability
Long history and selectivity of track recording – SSNTDs can retain a record of activity for billions of years	Poor charge and energy discrimination-track size/shape depends upon the charge and mass of the particles as well as the angle of incidence. There is significant overlap in the size distributions of the tracks due to energetic particles
Existence of thresholds for registration – SSNTDs can register particles only if their charge and LET value are above a threshold	Variability in SSNTDs – environmental conditions and manufacturing procedures results in problems of precision and reproducibility
Ruggedness and simplicity Inexpensive Integrating capability Can respond to both charged particles and neutrons	Lack of theoretical understanding – no theoretical work explains how certain properties of materials can predicate or ascertain a viable ability for track formation/retention

Investigators who have used CR-39 detectors in Pd/D electrolysis experiments include Oriani and Fisher [3], Roussetski [4], and Lipson et al. [5–7]. The experimental configurations employed and results are summarized in Table 2. Based upon the success of these earlier experiments, the use of CR-39 detectors in Pd/D co-deposition experiments was explored.

In the Pd/D co-deposition experiments, the tracks are concentrated in areas where the cathode was in contact with the CR-39 detector [8]. A comparison of tracks obtained from a known alpha source and those obtained as a result of Pd/D co-deposition is shown in Fig. 1. Figure 1(a) shows tracks obtained when a CR-39 detector is exposed to alphas from an ^{241}Am source. Tracks obtained as a result of Pd/D co-deposition are shown in Fig. 1(b). For the top images of Figs. 1(a) and (b), the microscope optics are focused on the surface of the detectors. The tracks are dark in color and either circular or oval in shape. When the microscope optics are focused on the bottom of the pits, bottom images of Figs. 1(a) and (b), a bright spot inside the track is observed. Tracks are conical in shape and the bright spot observed inside the track is due to the tip of the cone acting like a lens when the detector is backlit. As shown in Fig. 1, the features of the tracks obtained as a result of Pd/D co-deposition are consistent with those obtained for alpha-particle generated tracks. A series of control experiments were done that showed that the Pd/D co-deposition tracks were not due to radioactive contamination of the cell components nor to either chemical or mechanical damage [8]. Experiments were done placing 6 μm thick Mylar between the CR-39 detector and the cathode indicating that the majority of tracks on the front surface have energies on the order or 1–3 MeV [9]. These conclusions were supported by track modeling and analysis using linear energy transfer (LET) curves.

Table 2. Summary of CR-39 Results obtained by other investigators.

Experimental configuration	Results
Pd sheet foil, electrolysis in Li_2SO_4 in D_2O, CR-39 placed above and below Pd cathode [3]	Track density of electrolysis experiments (150–3760 tracks cm^{-2}) greater than controls (59–541 tracks cm^{-2})
Au/Pd/PdO heterostructures, load with D electrolytically, remove from cell and place in contact with CR-39, cycle temperature for 1 h [4]	Observed triple tracks due to the carbon breakup reaction. The number of tritons needed to create triple tracks greater than the yield of DD tritons.
Au/Pd/PdO heterostructures, load with D electrolytically, remove from cell and place in contact with CR-39, cycle temperature for 1 h [5]	Tracks detected in CR-39 that were consistent with 2.5–3.0 MeV protons and 0.5–1.5 MeV tritons
50 μm thick Pd foil, electrolysis in Li_2SO_4 in H_2O, CR-39 placed in contact with Pd cathode [6]	Tracks concentrated in areas where the cathode was in contact with the CR-39 detector
Thin Pd films, electrolysis in Li_2SO_4 in H_2O, Cu and Al spacers placed between CR-39 and Pd cathode [7]	Tracks in CR-39 detectors consistent with 11–16 MeV alphas and 1.7 MeV protons

In addition to tracks on the front surface of the CR-39 detectors, tracks have also been observed on the backside of the 1 mm thick detectors. In this communication, the nature of the tracks observed on the back surface of the CR-39 detectors are discussed.

2. Experimental Procedure

Cell assembly and experimental procedures have been described elsewhere [8,9]. In these experiments, the CR-39 detectors are placed in close proximity to the cathode, as illustrated in Fig. 2(a). This is due to the energy losses the particles sustain as they traverse through water. The deposit formed as a result of Pd/D co-deposition, Fig. 2(b), has a cauliflower-like morphology that traps pockets of water. Because of the morphology of the Pd deposit, the thickness of the water layer will vary. Linear energy transfer (LET) curves are used to determine how far an energetic, charged particle can travel through a medium of known composition and density. In this investigation LET curves were calculated using the SRIM-2003.26 code of Ziegler and Biersack [10]. This code can be downloaded from the http://www.srim.org/ website. The LET curves, shown in Fig. 2(c), illustrate the impact a thin water film, of varying thickness, has on the energy of the charged particles.

Prior to using a CR-39 detector in an experiment, one corner on the side facing away from the cathode is exposed to an ^{241}Am source. This provides an internal standard that can be used to account for variability in the CR-39 detectors. By having an internal standard on the same detector used in an experiment assures that both sets of tracks experience identical experimental and etching conditions. The track images shown in Fig. 1 were from the same CR-39 detector. At the completion of the experiment, the cell was disassembled and the CR-39 detector was etched in 6.5 N NaOH solution for 6 h at 62–68°C. After etching, the CR-39 detector was analyzed using either a Nikon Eclipse E600 microscope or an automated track analysis system.

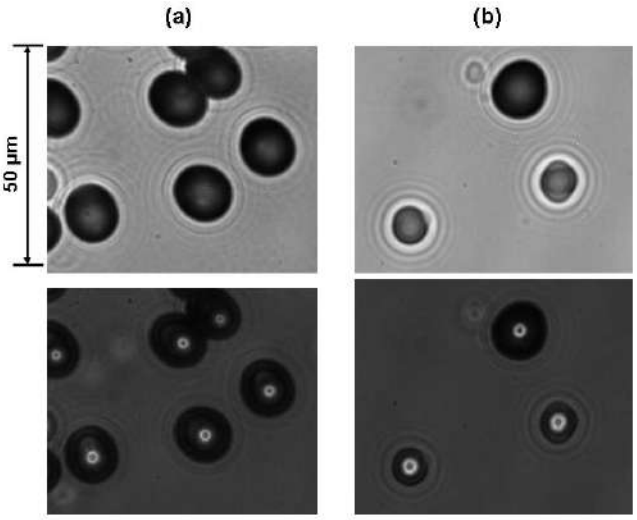

Figure 1. Images of tracks on CR-39 obtained (a) upon exposure to an americium-241 alpha source and (b) as a result of a Pd/D co-deposition experiment on a Au cathode. Both sets of tracks were on the same CR-39 detector. In the top images, the focus is on the surface of the CR-39 detector. The bottom images are an overlay of two images taken at two different focal lengths (top and bottom of pits).

3. Results and Discussion

3.1. Neutron interactions with CR-39 detectors

The possible interactions of DD neutrons (2.45 MeV) and DT neutrons (14.1 MeV) are described in Fig. 3(a). In the interaction shown in case 1, the DD and DT neutrons can scatter elastically, producing recoil protons, carbons, or oxygen nuclei in the forward direction. But DT neutrons can also undergo two inelastic (n,p) and (n,α) reactions with carbon or oxygen, cases 2 and 3, respectively, in Fig. 3(a). These inelastic reactions result in charged particles that can produce tracks on the front and/or the back surfaces of the CR-39 detector. Phillips et al. [11] have shown that neutron spectrometry can be done using CR-39. At low neutron energies (0.144 MeV), only recoil protons are seen and are observed as a peak at $\sim$10 μm neutron, Fig. 3(b). As the neutron energy increases, a broadening of the proton recoil peak at $\sim$10 μm is observed. At 1.2 MeV neutron energy, a second peak is visible at $\sim$25 μm. This second peak is attributed to recoil carbon and oxygen atoms. For neutron energies between 1.2 and 8 MeV, the size distributions of tracks observed in the CR-39 detectors are roughly similar. In the CR-39 detector exposed to 14.8 MeV neutrons, a decrease in the proton recoil at $\sim$10 μm is observed, Fig. 3(b), and a peak is observed at $\sim$35 μm which is attributed to the three alpha particle reactions.

3.2. Characterization of tracks observed on the backside of the CR-39 detectors

Earlier it was reported that tracks had been observed on the backside of a CR-39 detector at the end of a Pd/D co-deposition experiment [13]. The CR-39 detectors used in these experiments are 1 mm in thickness. The LET curves

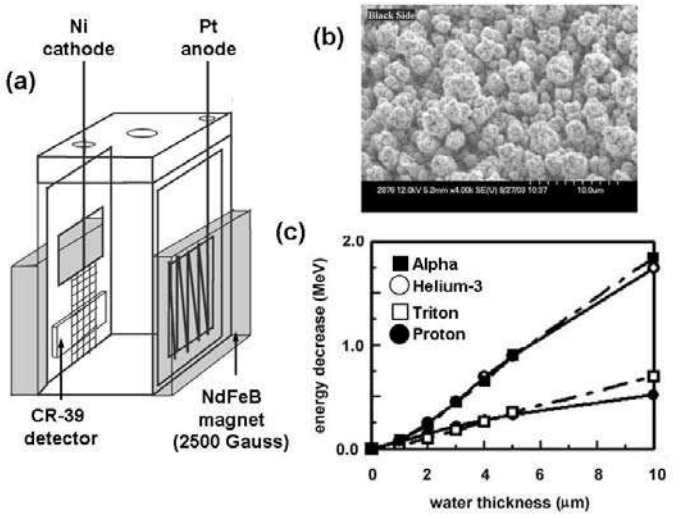

Figure 2. (a) Schematic of the cell showing the placement of the CR-39 detector. (b) SEM image showing the morphology of the Pd deposit created on a Au cathode as a result of Pd/D co-deposition. Reprinted with permission from *Eur. Phys. J. Appl. Phys.* [8]. (c) LET curves showing the decrease in energy of the charged particles as a function of water thickness.

indicate that the only particles that can traverse through 1 mm thick CR-39 are $\geqslant$40 MeV alphas, $\geqslant$10 MeV protons, and neutrons. Figure 4 shows the size distribution of the Pd/D generated tracks observed on the backside of the detector. The tracks range in size from 5 to 40 μm. A 40 MeV alpha would leave a $\sim$5.5 μm diameter track on the front surface of the detector [6]. A 10 MeV proton would leave a $\sim$ 1.7 μm diameter track on the front surface [14]. When a charged particle passes through a medium, it causes extensive ionization of the material [15]. The particle loses energy as it travels through the medium and eventually stops. As the particle loses energy and slows down, the extent of the damage caused by the ionization decreases. After etching, the resultant track has a conical shape. Consequently, the diameter of the track is largest on the surface where the particle entered the detector than inside where the particle stops. This indicates that the diameters of the 40 MeV alpha and 10 MeV proton generated tracks on the back surface of the CR-39 detectors will be significantly smaller than the diameters on the front surface. Since the track size distribution, shown in Fig. 4, ranges between 5 and 45 μm, it is unlikely that the observed tracks are due to $\geqslant$40 MeV alphas and $\geqslant$10 MeV protons.

In Fig. 4, the size distribution of the Pd/D generated tracks is overlaid with the size distributions of tracks obtained for CR-39 detectors exposed to 2.45 and 14.8 MeV neutrons. The peaks attributed to recoil protons, recoil carbon and oxygen, and carbon shattering are indicated. The 2.45 and 14.8 MeV neutrons are created by DD and DT fusion, respectively. The primary DD reactions and secondary DT and D^3He are:

$$D + D \rightarrow T\ (1.01\ \text{MeV}) + p\ (3.02\ \text{MeV}),$$

$$D + D \rightarrow n\ (2.45\ \text{MeV}) + {}^3He\ (0.82\ \text{MeV}),$$

$$D + T\ (\leqslant 1.01\ \text{MeV}) \rightarrow \quad \alpha\ (6.7\text{–}1.4\ \text{MeV}) + n\ (11.9\text{–}17.2\ \text{MeV}),$$

$$D + {}^3He\ (\leqslant 0.82\ \text{MeV}) \rightarrow \quad \alpha\ (6.6\text{–}1.7\ \text{MeV}) + p\ (12.6\text{–}17.5\ \text{MeV}).$$

As shown in Fig. 4, these neutrons can be differentiated simply by examining the size distribution of the tracks. Compared to DT fusion, the recoil proton peak observed for DD fusion is shifted to larger track size. The shift to larger track size is probably due to the fact that the DD neutrons are less energetic than the DT neutrons. The energy transferred to a proton is less when hit by a DD neutron than with a DT neutron. Less energy results in bigger tracks. For DT fusion, a peak is observed between 30 and 40 μm that is attributable to the carbon breakup reaction. This peak is absent in the DD fusion track size distribution. The size distribution obtained on the back side of a CR-39 detector that had been used in a Pd/D co-deposition experiment exhibits features consistent with both DD and DT fusion. Both the CR-39 track size distributions obtained for DT fusion and Pd/D co-deposition show tracks between 30 and 40 μm that are attributable to the carbon breakup reaction. This peak is absent in the DD fusion track size distribution. The recoil proton peak observed for the Pd/D co-deposition track size distribution has both a small track size (DT) and large track size (DD) contribution. These results suggest that both DD and DT fusion reactions are occurring. These conclusions are further supported by the Mylar experiments and the track modeling [16]. In these experiments a 6 μm thick Mylar spacer was placed between the CR-39 detector and the cathode. These experiments indicated that the majority of the charged particles leaving tracks on the front surface of the detector have energies on the order of 1–3 MeV. This energy range is consistent with the energies of charged particles formed as a result of the primary DD and secondary DT and D^3He reactions.

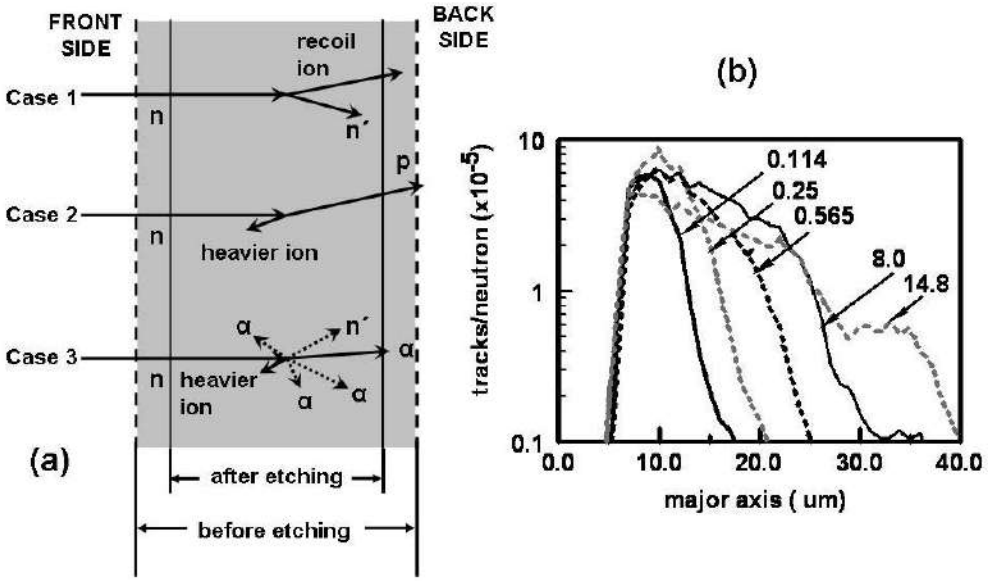

Figure 3. (a) Schematic drawing of the CR-39 track detector and the neutron interaction processes that can take place inside the plastic [12]. The drawing is not to scale. Case 1 summarizes the DD neutron interaction with CR-39. Cases 1–3 describe the DT neutron interactions with CR-39. Reprinted with permission from Naturwissenshaften [17]. (b) Track size distribution for CR-39 detectors that have been exposed to neutrons [11]. The energies of the neutrons, in MeV, are indicated.

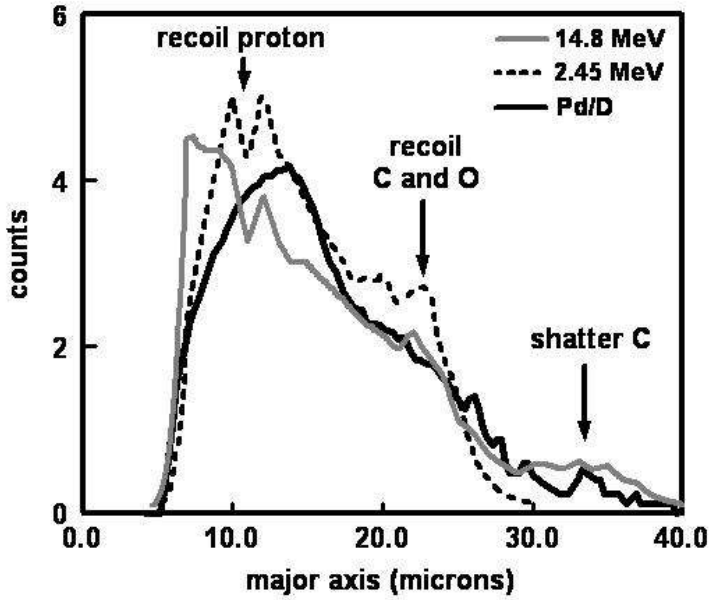

Figure 4. Track size distribution for CR-39 detectors that have been exposed to 2.45 and 14.8 MeV neutrons are overlaid with the track size distribution obtained on the backside of a CR-39 detector used in a Pd/D co-deposition experiment.

3.3. Visual comparison of Pd/D tracks with neutron generated tracks and the results of sequential etching

A photomicrograph of tracks observed on the backside of a CR-39 detector that was used in a Pd/D co-deposition experiment, Fig. 5(a), is compared with a photomicrograph of tracks resulting from exposure to a ^{238}PuO, broad-spectrum neutron source, Fig. 5(b). In both photomicrographs, it can be seen that the tracks are primarily circular in shape. However, some tracks are circular with a small tail, indicated by arrows in Figs. 5(a) and (b). These are recoil protons that have exited the CR-39 at a angle less than 90°. Small tracks are also observed in these photomicrographs. Some of these smaller tracks are indicated by a circle in Figs. 5(a) and (b).

As illustrated in Fig. 3(a), neutron interactions can occur anywhere throughout the CR-39 detector. These smaller tracks are attributed to tracks that are deeper inside the CR-39 detector. These latent tracks can become prominent with additional etching of the CR-39 detectors, as shown in Figs. 5(c) and (d). In Fig. 5(c), three very large tracks are observed. These tracks originally appeared on the surface of the detector after the first etch. After additional etching these three tracks got much larger. The lower two tracks have pear-like shapes with tails. These features indicate that the particles that created these tracks came in at an oblique angle. These two tracks are lighter in color than the top track. This indicates that the bottom two tracks are shallower than the top track. Again this indicates that the particles that created these tracks came in at an oblique angle. In contrast, the top track is circular in shape and is much darker in color than the other two surface tracks. These features are consistent with a particle entering the detector at a ∼90 ° angle. To the left of this track, a much smaller track is observed that is elliptical in shape. This smaller track resulted

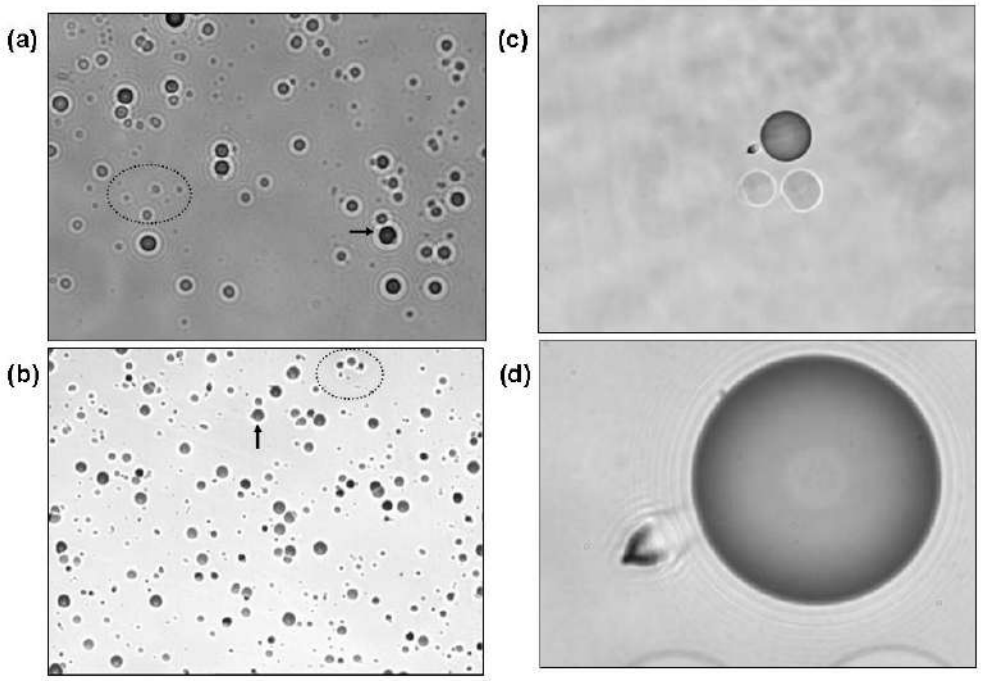

Figure 5. Photomicrograph of tracks observed (a) on the backside of a CR-39 detector used in a Ag/Pd/D co-deposition, magnetic field experiment and (b) on a CR-39 detector exposed to neutrons from a ^{238}PuO source (image supplied by Gary Phillips). Magnification 200×. Latent tracks are circled. Arrow indicates circular tracks with a small tail. Results of sequential etching of the CR-39 detector where (c) was taken at a magnification of 200x and (d) was taken at a magnification of 1000x.

from a neutron hitting an atom deeper inside the detector. Given the size and shape of this track, it is most likely a recoil proton moving in the forward direction and resulted from the reaction shown in case 1 of Fig. 3(a).

3.4. Triple tracks–evidence of energetic neutrons

Figure 6(a) shows tracks obtained in a Pd/D co-deposition experiment in which a 60 μm thick polyethylene film was placed between the cathode and the CR-39 detector. Besides neutrons, the LET curves indicate that >2 MeV protons and >10 MeV alphas can penetrate 60 μm thick polyethylene. In Fig. 6(a), a triple track is observed among the solitary tracks. As the density of tracks in this region is low, it is unlikely that this triple track is due to overlapping tracks. Examination of the bottom of the track, Fig. 6(b), shows three individual lobes breaking away from a center point. It is unlikely that such a structure would be observed for three tracks that overlap randomly. A triple track, such as the one shown in Fig. 6, is indicative of a reaction resulting in the formation of three particles of equal mass and energy. This reaction is the carbon break up reaction illustrated in case 3 in Fig. 3(a) and provides additional evidence of the emission of neutrons by the Pd/D system [17]. In the carbon breakup reaction, an energetic neutron creates a metastable ^{13}C atom in the CR-39 detector, which then shatteres into three alpha particles. The residuals of this reaction can be viewed in the CR-39 detector as a three-prong star where each prong represents each charged particle that occurs in the

decay [18].

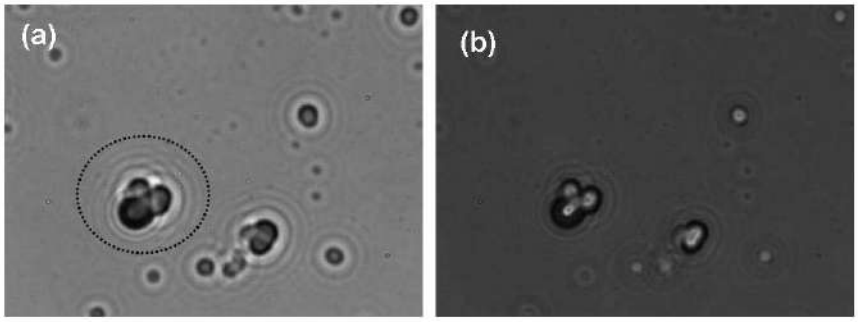

Figure 6. (a) Image of a triple track (circled) among solitary tracks on a CR-39 detector used in a Au–Ag–Pt three wire experiment done in the presence of a magnetic field. (magnification 1000×). In this experiment, a 60 μm thick piece of polyethylene was between the detector and the cathodes. This photomicrogragh was obtained by focusing the optics on the surface of the detector. (b) Overlay of two photomicrographs taken at different focal lengths (surface and bottom of the pits).

Figure 7(a) shows another triple track. This triple track was created in a Pd/D co-deposition experiment in which the cathode was in direct contact with the CR-39 detector. Looking inside the track, Fig. 7(b), it can be seen that the alpha track designated α_3 is separated from the other two tracks. The threshold energy of the neutron required to shatter a carbon atom to form a three-prong star is 9.6 MeV [19]. Knowing the threshold energy needed to shatter a carbon atom and the distance each alpha particle of the triple track has traveled in the detector, the energy of the neutron that created that triple track can be estimated. The LET curve shown in Fig. 7(c) is used to determine the stopping distance of alphas in CR-39 as a function of alpha-particle energy. The energy of the neutron is given by the following relationship:

$$E_{\mathrm{n}} = E_{\mathrm{th}} + E_{\alpha 1} + E_{\alpha 2} + E_{\alpha 3}, \tag{1}$$

where E_{n} and E_{th} are the energy of the neutron causing the triple track and threshold energy required to shatter a carbon atom, respectively, and $E_{\alpha 1}$,$E_{\alpha 2}$, and $E_{\alpha 3}$ are the energies of the alpha particles. In Fig. 7(b), the distance between the center point and the prongs of the triple track are indicated. Using the LET curve, Fig. 7(c), these distances can be converted into energy. The energies of the alphas are therefore 0.6, 0.9, and 1.2 MeV. The threshold energy of a neutron to shatter a carbon atom is 9.6 MeV. Adding these energies together, the energy of the neutron that created the triple track shown in Fig. 7 is estimated to be 12.3 MeV. In DT fusion reactions, the neutron has an energy ranging between 11.9 and 17.2 MeV.

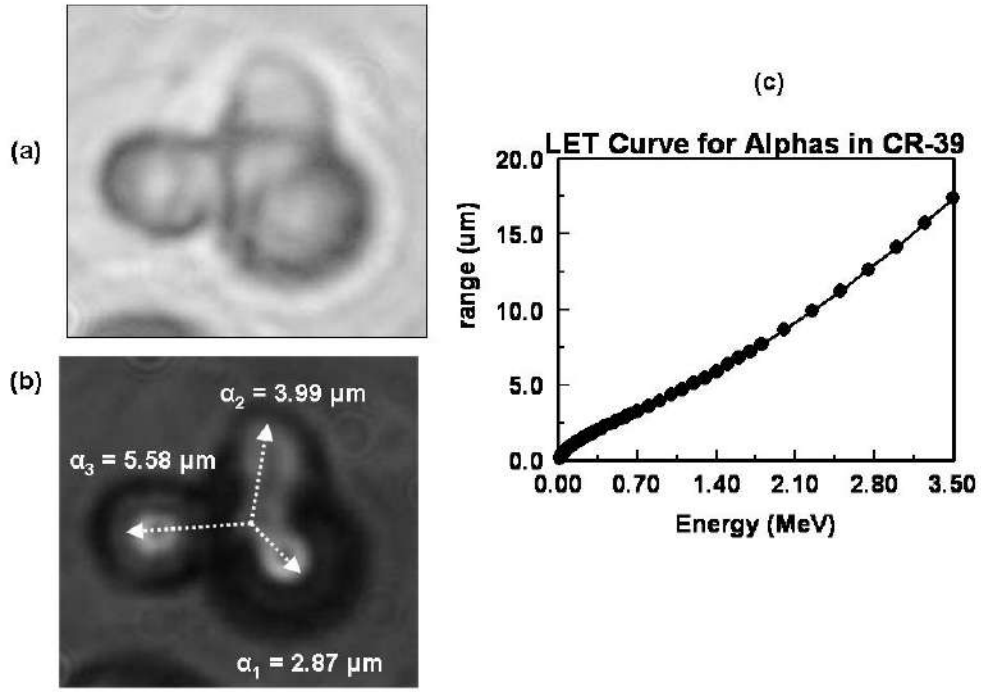

Figure 7. (a) Photomicrograph of a triple track obtained with the optics focused on the surface of the CR-39 detector. Reprinted with permission from Naturwissenshaften [17]. (b) Overlay of two photomicrographs taken at different focal lengths (surface and bottom of the pits). (c) LET curve for alphas in CR-39.

4. Conclusions

CR-39 detectors have been used to monitor the nuclear processes occurring inside the Pd lattice created as a result of the Pd/D co-depoition process. In these experiments, tracks have been observed on both the front and back surfaces of the CR-39 detectors. Mylar spacer experiments, track modeling, and LET curves indicate that the majority of the charged particles on the front surface have energies between one and three MeV. This energy range is consistent for charged particles produced as the result of DD primary fusion reactions. Sequential etching of the CR-39 detectors shows the presence of tracks deeper inside the plastic that are attributable latent tracks due to neutron interactions. Tracks on the backside of the CR-39 detectors range in size between five and forty microns. This size distribution is consistent with neutrons resulting from both DD primary and secondary fusion reactions. The presence of triple tracks, attributable to the carbon breakup reaction, provides additional evidence of neutrons with energies greater than 9.6 MeV. Such neutrons can be formed as the result of DT secondary reactions.

Acknowledgements

This work was funded by the Defense Threat Reduction Agency (DTRA) and JWK Corporation. The authors would like to thank Dr. Gary Phillips, nuclear physicist, retired from the Naval Research Laboratory, US Navy, Radiation

Effects Branch, for valuable discussions in interpreting the data. The authors acknowledge the contributions of Dr. Stanislaw Szpak, who pioneered the Pd/D co-deposition process.

.

References

[1] B.G. Cartwright, E.K. Shirk and P.B. Price, A nuclear-track-recording polymer of unique sensitivity and resolution, *Nucl. Instru. Meth.* **153 1978** (1978) 457–460.
[2] S.A. Durrani, Nuclear Tracks today: strengths, weaknesses, challenges, *Rad. Measurements* **43** (2008) S26–S33.
[3] R.A. Oriani and F.C. Fisher, Generation of nuclear tracks during electrolysis, *Jpn. J. Appl. Phys.* **41** (2002) 6180–6183.
[4] A.S. Roussetski, Application of CR-39 plastic track detectors for detection of DD and DT-reaction products in cold fusion experiments, in *Condensed Matter Nuclear Science: Proceedings of the 8th International Conference on Cold Fusion*, Lerici, La Spezia, Italy, 2000.
[5] A.G. Lipson, B.F. Lyakhov, A.S. Roussetski, T. Akimoto, T. Mizuno, N. Asami, R. Shimada, S. Miyashita and A. Takahashi, Evidence of low-intensity D–D reactions as a result of exothermic deuterium desorption from Au/Pd/PdO:D heterostructure, *Fussion Technol.* **38** (2000) 238–252.
[6] A.G. Lipson, A.S. Roussetski, G.H. Miley and C.H. Castano, In-situ charged particles and X-ray detection in Pd thin film-cathodes during electrolysis in Li_2SO_4/H_2O, in *Condensed Matter Nuclear Science: Proceedings of the 9th International Conference on Cold Fusion*, Beijing, China, May 19–24, 2002; X.Z. Li (Ed.), Tsinghua Univ. Press, Beijing, 2002, pp. 218–223.
[7] A.G. Lipson, A.S. Roussetski, G.H. Miley and E.I. Saunin, Phenomenon of an energetic charged particle emission from hydrogen/deuterium loaded metals, In *Condensed Matter Nuclear Science: Proceedings of the 10^{th} International Conference on Cold Fusion*, Cambridge, MA, Aug. 24–29, 2003, P.L. Hagelstein and S.R. Chubb (Eds.), World Scientific, Singapore, 2006, pp. 539–558.
[8] P.A. Mosier-Boss, S. Szpak, F.E. Gordon and L.P.G. Forsley, The use of CR-39 in Pd/D co-deposition experiments, *Eur. Phys. J. Appl. Phys.* **40** (2007) 293–303.
[9] P.A. Mosier-Boss, S. Szpak, F.E. Gordon and L.P.G. Forsley, Reply to comment on the use of CR-39 in Pd/D co-deposition experiments: a Response to Kowalski. *Eur. Phys. J. Appl. Phys.*, **44** (2008) 291–295.
[10] J.F. Ziegler and J.P. Biersack, *The Stopping and Range of Ions in Solids*, 1985.
[11] G.W. Phillips, J.E. Spann, J.S. Bogard, T. VoDinh, D. Emfietzoglou, R.T. Devine and M. Moscovitch, Neutron spectrometry using CR-39 track etch detectors, *Radiation Protection Dosim.* **120** (2006) 457–460.
[12] J.A. Frenje, C.K. Li, F.H. Séguin, D.G. Hicks, S. Kurebayashi, R.D. Petrasso, S. Roberts, V.Y. Glebov, D.D. Meyerhofer, T.C. Sangster, J.M. Soures, C. Stoeckl, G.J. Schmid and R.A. Lerche, Absolute measurements of neutron yields from DD and DT tmplosions at the OMEGA laser facility using CR-39 track detectors, *Rev. Sci. Instrum.* **73** (2002) 2597–2605.
[13] P.A. Mosier-Boss, S. Szpak, F.E. Gordon and L.P.G. Forsley, Detection of energetic particles and neutrons emitted during Pd/D co-deposition, *Low-Energy Nuclear Reactions Sourcebook,* 2008.
[14] F.H. Séguin, J.A. Frenje, C.K. Li, D.G. Hicks, S. Kurebayashi, J.R. Rygg, B.-E. Schwartz, R.D. Petrasso, S. Roberts, J.M. Soures, D.D. Meyerhofer, T.C. Sangster, J.P. Knauer, C. Sorce, V.Y. Glebov, C. Stoeckl, T.W. Phillips, R.J. Leeper, K. Fletcher and S. Padalino, Spectrometry of charged particles from inertial-confinement-fusion plasmas, *Rev. Sci. Instrum*. **74** (2003) 975–995.
[15] D. Nikezic and K.N. Yu, Formation and growth of tracks in nuclear track materials, *Mat. Sci. Eng. R.* **46** (2004) 51–123.
[16] P.A. Mosier-Boss, S. Szpak, F.E. Gordon and L.P.G. Forsley, Characterization of tracks in CR-39 detectors obtained as a result of Pd/D co-Deposition, *Eur. Phys. J. Appl. Phys.* **46** (2009) ?????.
[17] P.A. Mosier-Boss, S. Szpak, F.E. Gordon ad L.P.G. Forsley, Triple tracks in CR-39 as the result of Pd-D co-deposition: evidence of energetic neutrons, *Naturwissenschaften* **96** (2009) 135–142.
[18] B. Antolkoviæ and Z. Dolenec, The neuton-induced ^{12}C(n,n')3α reaction at 14.4 MeV in a kinematically vomplete experiment, *Nuclear Phys. A* **237** (1975) 235–252.
[19] S.A.R. Al-Najjar, A. Abddel-Naby and S.A. Durrani, Fast-neutron spectrometry using the triple-α reaction on the CR-39 detector, *Nuclear Tracks* **12** (1986) 611–615.